Crack Path Development and Related Safety Considerations for Heavy Duty Railroad Wheels

H.P. Rossmanith[1], F. Loibnegger and R. Huber[2]

[1] Institute of Mechanics & Mechatronics, Wiedner Hauptstr. 8-10/325, A-1040 Vienna, Austria; hans.peter.rossmanith@tuwien.ac.at
[2] Institute for Testing and Research in Materials Technology, Karlsplatz 13, A-1010 Vienna, Austria; friedrich.loibnegger@tuwien.ac.at and richard.huber@tuwien.ac.at.

ABSTRACT

This contribution presents a hybrid analytical-numerical analysis of the thermo-mechanical fatigue behavior of heavy duty railway wheels. The wheels were repeatedly frictionally disk-braked at random sequences of time instants. As the loading was rather severe, the stresses during braking and subsequent cooling reached the plastic limits in compression and tension, respectively. Hence, the initiation and propagation of fatigue cracks was observed. This paper addresses the behavior of these cracks under severe service conditions including residual stresses, and discusses the conditions for fatigue crack extension as well as the possibility to arrest these cracks. Finally safety issues and safe life time diagrams are presented.

1. INTRODUCTION

In the disk-braking process of rotating machinery, such as rolling wheels of railways, the kinetic energy is mainly converted into heat within a relatively short time. During disk braking the brake pads are in sliding frictional contact with the rotating disk. As the brake pads usually cover only a part of the annular brake area one has a periodic transient heat production over a sector of the brake surface. If the disk rotates at a rather high spinning rate and, in addition, differential heat transfer to neighbouring sections of the brake annulus is basically negligible during one revolution of the disk, one can safely assume that heat production occurs uniformly within the circumferential annular ring area. The distribution of heat production along a radial line within the brake annulus depends on the sliding velocity, which increases linearly, and the contact force. The contact force is controlled by the design of the brake pads and to a lesser degree also changes during braking due to the thermal deformation of the heat input region. Under certain circumstances, hot bands and/or hot spots may develop within the brake region and they may lead to a highly non-uniform heat production and resulting temperature distribution [1].

2. BRAKING A ROLLING RAILWAY WHEEL

In this paper the heavy duty railway wheel is modelled as an isotropic thermo-elasto-plastic disk of diameter D and thickness B where, as shown in Fig. 1, $B = D \xi /2$ where $\xi \approx$ ½. A cylindrical co-ordinate system (r, θ, z) is located in the centre of the disk and the side surfaces are defined by (r, θ; z = ± B/2). The disk rotates with angular velocity ω. Braking occurs on both sides of the disk within an annulus determined by ($r_i = D_{B1}/2 \leq r \leq r_a = D_{B2}/2$; z = ± B/2).
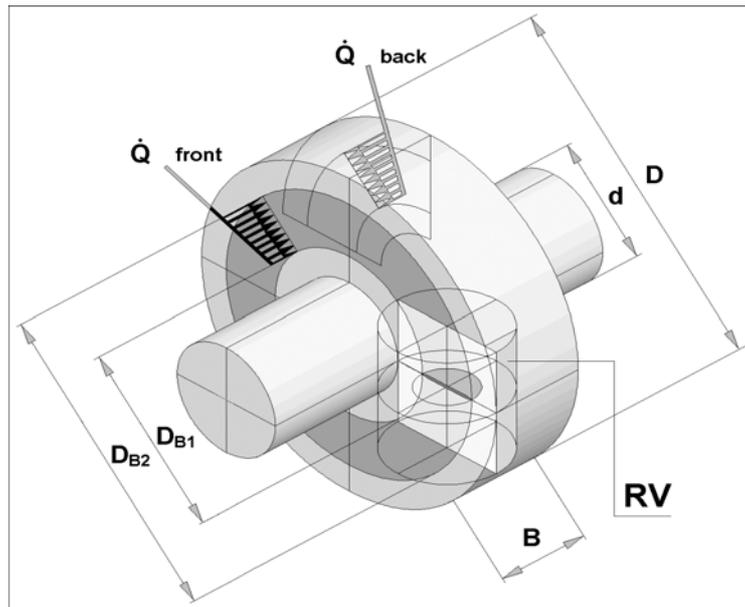
Fig. 1: Shaft with shrink-fitted disk: geometry, thermal loading

2.1 Thermal considerations

During braking the kinetic energy of the rolling wheel is partially or completely converted into sliding frictional energy, i.e. into heat and deformation (elastic and possibly plastic). The analysis rests upon the general assumption, that the total amount of brake energy is supplied to the wheel. The heat Q, simulated by a linear profile and generated by frictional forces in the annular zone ($r_i = D_{B1}/2 \leq r \leq r_a = D_{B2}/2$) flows into the body of the disk across the front and back sliding contact area where it generates a rather complicated time-varying, inhomogeneous temperature distribution. The thermal energy - flowing through the wheel and the axis - is radiated and conducted across the free surfaces to the ambient air volume. Contrary to reality, it is assumed that the brake pads do neither absorb nor supply thermal energy to the brake system.

Due to the non-uniform heat flow, dQ/dt, different points in the body will experience their extreme values of the temperature field at different times. The disk is not insulated and may loose heat all across its surface and also through the axle. It is assumed that, before braking occurs, the spinning disk is at uniform reference temperature T_o.

Usually the disk will be fixed on an axle either by thermal shrink fitting or by pressing the disk on a weakly conical section of the axle. In both cases, the result is the formation of a mechanical residual stress field Σ_o^* $\{\sigma_o{}^*{}_r, \sigma_o{}^*{}_\theta, \sigma_o{}^*{}_z\}$, basically characterized by radial and circumferential tensile stresses in the disk. This non-zero initial residual stress field is usually locked-in and must be superimposed to the thermal stresses. Here, these mechanical shrink-fit stresses were taken into account via Boot's-conversion method in the form of suitably distributed thermal sources and sinks.

As the heat flow during braking causes the temperatures in the rim and hub to be lower than in the central zone, the resulting severe constraint prevents the disk from expanding in the radial direction. This radial constraint induces a circumferential constraint which causes large compressive stresses to be built up during heat production which must be balanced by tensile circumferential stresses in the rim of the disk.

All material parameters strongly vary with temperature. Young's modulus, E, and the tensile linear elastic limit, $R_{po,2}$, decrease with temperature, whereas the linear expansion coefficient, α, increases with temperature. In addition, the yield strengths in tension and compression also depend on the temperature. Changes in the microstructure of certain materials, when loaded above critical levels of temperature, have been neglected in the analysis.

2.2 Brake events and sequencing

The evolution of thermal stresses in the disks depends strongly on the number and sequence of the individual brake events. In many cases, the brake events may follow each other so closely in time, that the time for cooling of the wheel surfaces within the brake annulus is too short for complete recovery of the initial thermal conditions. In these cases, thermal energy is built up within the wheel and the general level of temperature rises continuously, randomly interrupted by the cooling periods. In this paper repetitive complete braking is assumed to occur, i.e. within a single brake event the wheel is frictionally decelerated to complete standstill. When - in practical applications - a series of brake events forms a brake sequence, the decay of the thermal stresses does not occur instantaneously but as a function of time, despite the fact that the mechanical stresses and strains form and decay instantaneously. Understandably, the sequence of brake events plays an important role in the accumulation and transfer of heat into the wheel as well as with respect to the response of the material, particularly, if the wheel is weakened by a deficiency such as a crack.

2.3 Heat production and temperature fields

Brake events of twenty minutes duration with fully frictional deceleration and uniform 12 kW heat through-put across the brake contact area was assumed. Heat conduction outside the brake surface was assumed to be 50 W/m K for an ambient temperature of 0°C. For the discussion of the results it is advantageous to define the *maximum temperature* within the disk. The location where the maximum temperature occurs may change as a function of time, and does not necessarily occur at a surface point.

Overall, however, the maximum temperature occurs in the smallest and thinnest disk and decreases with increasing diameter and increasing thickness [2].

2.4 Stress fields after braking and cooling

Before surface crack formation in the brake area the problem is rotationally symmetrical and a two-dimensional finite element analysis is appropriate. The distribution of the temperature, T, and the circumferential stress, σ_θ, at the end of braking (when the entire heat energy has been transferred to the disk) indicates that for a given heat energy input, the smallest disk exhibits the highest temperature which is located on the surface in the central section of the brake area. The temperature distribution decays rapidly with increasing depth from the surface. At the end of heat input by braking, for all sizes and thicknesses of disks investigated, the circumferential stresses are compressive.

At the end of braking the brake pads are instantly completely removed and the disk is allowed to cool down to ambient temperature (which in the present case was 0°C). Figure 2 shows the distribution of the circumferential stress σ_θ at the end of the cooling phase as a function of the radial coordinate across the brake area. The most eye-catching feature is the extremely large amplitude of the residual tensile stress in the central region of the brake area for the thinnest and smallest disk (A1). This stress is 635 MPa and thus 5% larger than the $R_{p0,2}$ value of 600 MPa of the material. Hence, plastic yielding is expected to occur at this site. This plastic zone is confined to a shallow layer beneath the surface, about 10 mm of thickness (see right hand side diagram in Fig. 2).
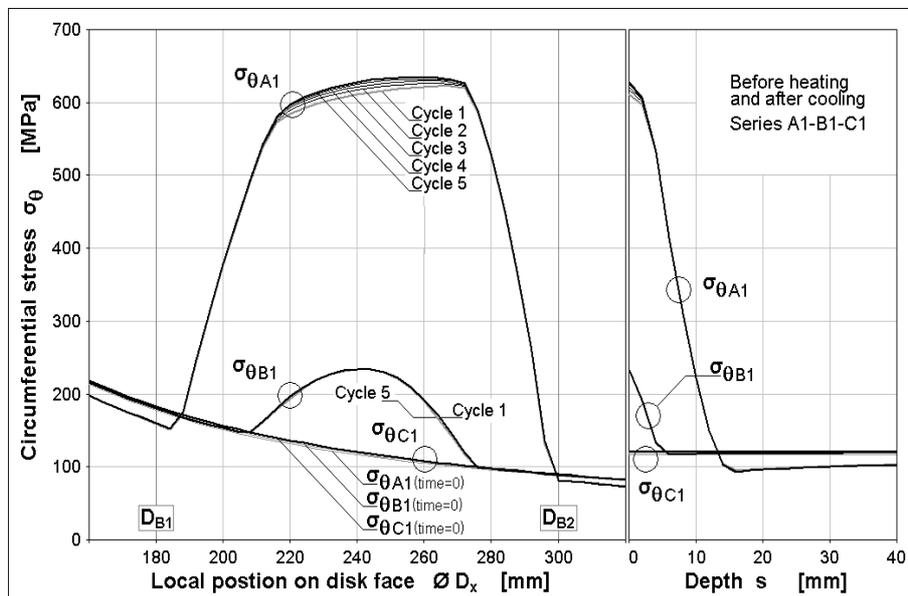
Fig. 2: Stresses in brake surface after cooling for various types of disks (A1, B1, C1 with increasing disk-diameter)

For comparison the values of the initial stress field, i.e. at time t=0, are also presented in Figure 2 (lower curve). These diagrams unveil the fact, that the residual stress field is

tensile and monotonically gently decreasing between 170 MPa at the inner boundary to about 80 MPa at the outer boundary of the brake area.

3. FATIGUE FRACTURE MECHANICS ANALYSIS

A set of radial surface cracks in the brake region of a heavy duty railway wheel is shown in Figure 3a. Figure 3b shows the depth extensions of crack No. 2 in Fig. 3a.
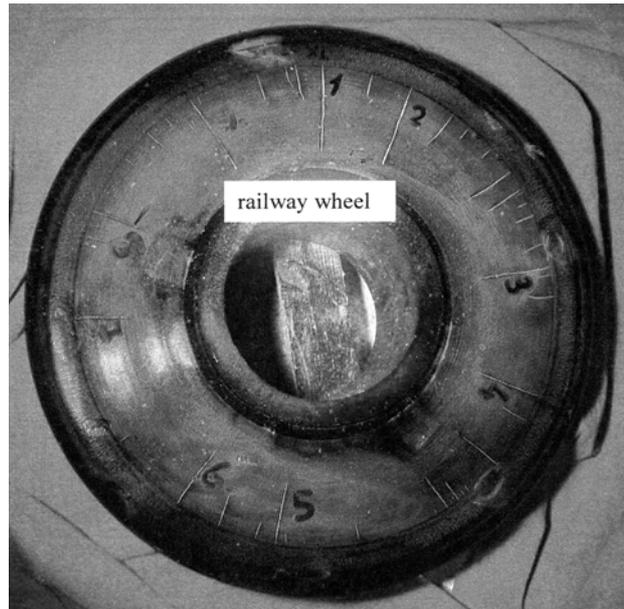
Fig. 3a: Set of radial surface cracks in a heavy duty railway wheel detected by non-destructive testing (MT) after service

Fig. 3b: Crack path of crack no. 2 in Fig 3a

Surface flaws incubating in the central region of the brake region mature into semi-elliptically shaped fatigue cracks which grow and extend in axial-radial planes. In order

to reach an acceptable solution of this rather difficult fracture problem, a few simplifying - but reasonable - assumptions had to be made for analysis purposes [2].

3.1 Crack modelling and determination of stress intensity factors

Crack modeling was achieved by first simulating the 3D problem as a rotationally symmetrical problem with a circular crack of radius 'a' positioned at the center of a cylindrical specimen indicated in Figure 1. Then, the stress intensity factor for the complex but rotationally symmetrically stress field (Biot-converted thermal as well as mechanical) was calculated. Next, by employing suitable correction functions, the stress intensity factors for the surface breaking points (C in Figure 4a) and the maximum depth point (point A in Figure 4b) of a semi-elliptical crack subjected to the real loading were calculated from known fracture mechanics formulae. As the stress distribution along the surface is very much different from the distribution along the depth direction, the stress intensity factors for points C and A were strikingly different. For details of the stress intensity factor calculation please consult Refs. [2, 3].

3.2 Fatigue crack propagation analysis and life time calculation

A fatigue crack propagation analysis on the basis of linear fracture mechanics was executed for a large number of cycles encompassing a sequence of individual phases such as decelerating the rolling wheel by breaking to complete standstill, cooling to ambient temperature, and accelerating again to initial conditions for the next cycle.

Experimentally determined da/dN data for rail wheel, $m = 5$ and $C = 1\ 10^{-18}$ in the [mm – Nmm$^{-3/2}$] system, were used. Data in a SIF band between $\Delta K = 250$ N/mm$^{3/2}$ (7,9 MPa√m) and $\Delta K = 650$ N/mm$^{3/2}$ (20,6 MPa√m) were regressed by a straight line. The *Paris law* in the form $dL/dN = C(\Delta K)^m$ was employed, where L stands for the surface extension '2c' or depth 'a' of the crack, N is the number of cycles, and ΔK is the variation of the stress intensity factor which is related to the stress variation. The stress variation $\Delta\sigma$ is the difference between the upper (tensile) stress level and the lower (tensile) stress level. Here, the lower stress level was taken to be zero because compressive stresses do not contribute to the SIF. Hence, the stresses vary between the maximum value after cooling (largest tensile circumferential stress) and zero at the time of brake release.

Integrating the *Paris equation* between the lower (a_0 = initial depth and $2a_0$ = surface extension of the crack; N = 0) and upper limit (a = current crack radius; N = current number of cycles) yields the current radius of the crack (a) as a function of the number of cycles, N.

It is to be noted that, in the basic numerical model, during crack extension the circular shape of the crack will be retained, but after modification for the semi-circular surface crack the fatigue crack extension speed becomes different for crack extension along the surface and into the depth. Hence, modification of the model yields different extension velocities for the crack extension along the surface and into the depth, hence, the shape of the crack will change into an ellipse with time-varying aspect ratio, 2c/a.

4. RESULTS AND DISCUSSION

The results for the stress intensity factors K_C (surface point) and K_A (depth point), the surface (2c) and depth (a) extensions of the crack, and the rates of crack extension along the surface (d(2c)/dN) and into the material (da/dN) are presented in Figures 4a and 4b. The initial crack surface extension $2c_0$ has been chosen to be 10 mm, the initial depth was $a_0 = 5$ mm. Results indicate that the crack extends primarily along the surface with a very slow increase in depth. This is also expressed by the fact that the scales along the abscissa in Figures 4a and 4b differ appreciably!

While along the surface the crack length advances only slightly during the first 2000 thermal cycles, the crack advance increases considerably during the next 2000 cycles. The crack length then increases at an average almost linear with doubling of the crack length from N = 2400 to N = 4800 cycles. Starting at about N = 5000 thermal cycles on the crack advances rapidly with ensuing fracture as soon as K_C reaches the value of the fracture toughness [K_{Ic} = 2000 N/mm$^{3/2}$ (63,2 MPa√m)]. The corresponding graphs for the deepest point, A, of the crack are given in Figure 4b. During the period of 5000 thermal cycles, both, the stress intensity factor and the crack velocity, decrease and, thus, the crack depth increases only slightly.
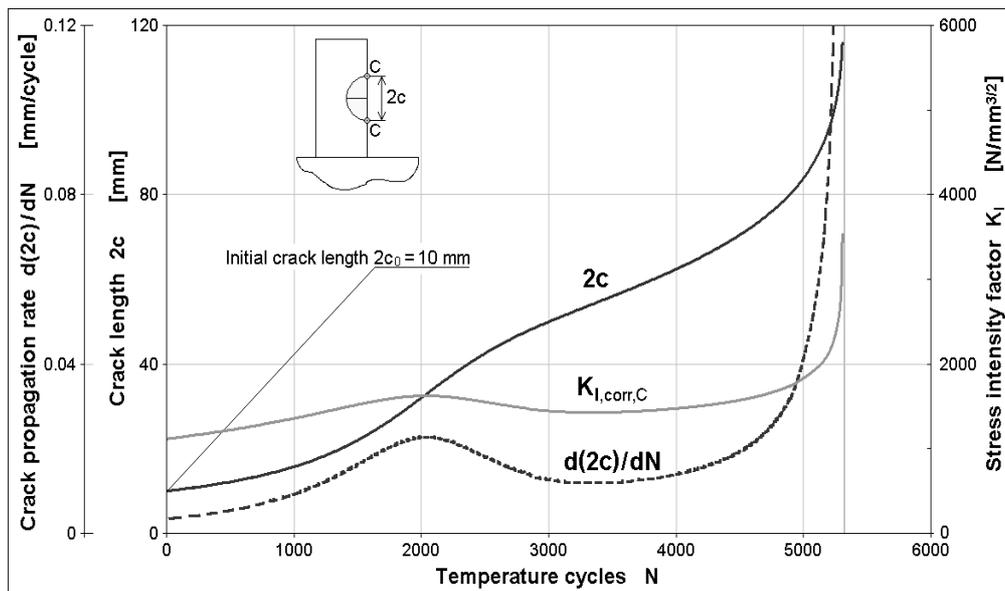
Fig. 4a: Crack extension along surface, point C

The effect of random loading and random braking as well as the influence of residual initial stresses will be treated in a forthcoming publication. From these data, diagrams were constructed for travel distance versus crack length for various numbers of brake events per 100 km. Results shown in Figure 5 indicate very slow crack extension in the depth direction but very fast extension along the surface. The addition of the residual stresses in the rim will arrest the crack at the edge of the brake area.
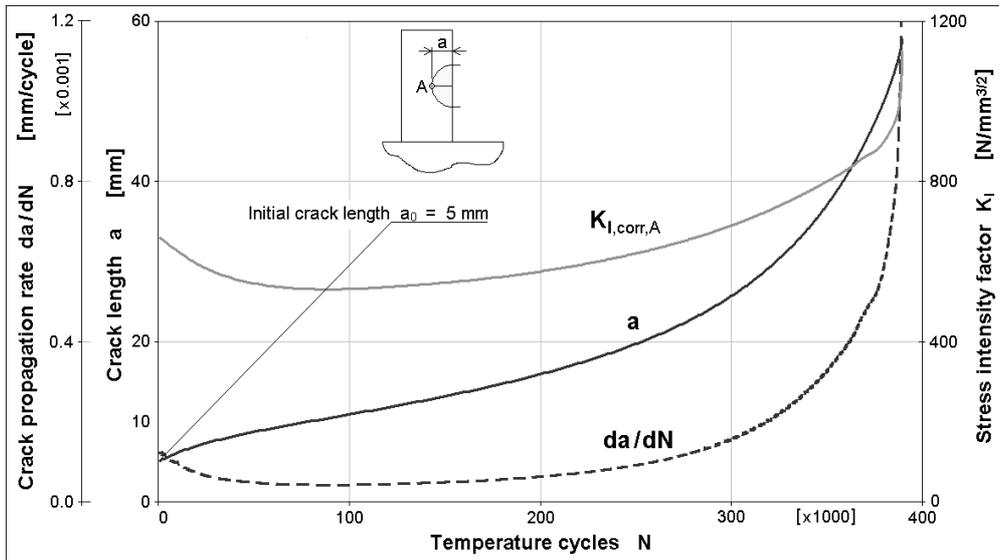
Fig. 4b: Crack extension in the depth direction, point A
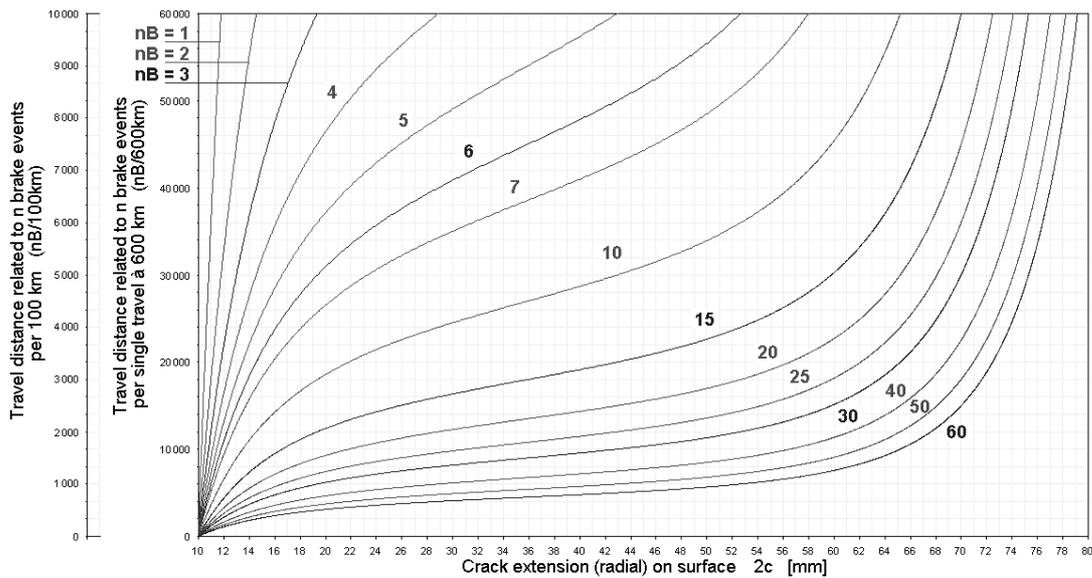
Fig. 5 Travel distance versus crack extension for various numbers of brake events

References

1. Gupta, V., G.T. Hahn, P.C. Bastias & C.A. Rubin (1996) Calculations of the frictional heating of a locomotive wheel attending rolling plus sliding. *Wear* 191:237-241.
2. Loibnegger, F., Rossmanith, H.P. & Huber, R., (2006) A thermo-mechanical model for fatigue fracture due to repeated braking of machine components. *Proc. of Conference ECF 16*, July 2006, Alexandropoulis, Greece (in print).
3. Rolfe S.T. & Barsoum, J.M. (1977) *Fracture and Fatigue Control in Structures - Applications of Fracture Mechanics*. Prentice-Hall, Inc., New Jersey.